Whole Earth Full-Waveform Inversion With Wavefield Adapted Meshes

Solvi Thrastarson* · Dirk-Philip van Herwaarden · Lion Krischer · Christian Boehm · Martin van Driel · Michael Afanasiev · Andreas Fichtner
Department of Earth Science, Institute of Geophysics, ETH Zürich
*soelvi.thrastarson@erdw.ethz.ch

1. Key Points

- We present a novel Full-Waveform Inversion (FWI) method that may reduce the computational cost of traditional FWI by an order of magnitude.
- The method is based on the usage of wavefield adapted meshes with anisotropic adaptive mesh refinements (aAMR).
- The range of applicability is limited but within this range the benefits are great.
- We show synthetic 2-D and 3-D proof of concept examples, which demonstrate the benefits of wavefield adapted meshes in FWI.
- We present the resulting model of a fully automatic prototype inversion using the presented methodology.

2. Wavefield Adapted Meshes

- Spectral-element meshes are designed to fit a certain number of gridpoints per wavelength.
- Wavelength is direction dependent. The azimuthal wavelength is longer than the radial one.
- Given a smooth medium and a source location, the pattern of propagation is roughly known before simulating.
- The azimuthal elements can thus be elongated, reducing the number of required elements to mesh the wavefield.
- The adjoint simulation has other source locations than the mesh is designed for and the adjoint wavefield is thus not a physical wavefield.
- That is however not a requirement to calculate a gradient as demonstrated on Figure 1.

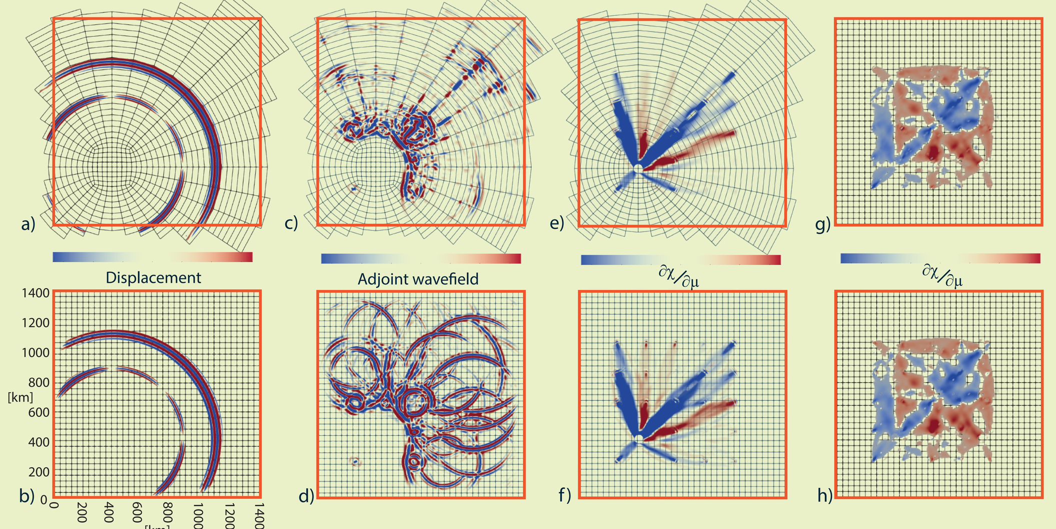

Figure 1. a) and b) show forward propagating wavefield simulated using the aAMR mesh and the Cartesian grid respectively.
c) and d) show the corresponding adjoint simulations using 25 adjoint sources.
e) and f) show the gradients calculated by correlating the backpropagated forward wavefields with the adjoint wavefields.
Finally g) and h) show summed gradients from 9 different sources. The aAMR gradients have been interpolated to a Cartesian grid and then summed.

3. Range of Applicability

- The wavefield adapted meshes work well when the used data is primarily transmissive waves.
- With a sharp reflective boundary present, the assumption behind the meshes is not valid anymore as the roughly circular/spherical pattern of propagation breaks (Figure 2).
- In three dimensions, this reflective boundary needs to be non-spherical to break the symmetry.
- When the medium is smooth, the meshes perform well (Figure 2).
- In regional to global scale FWI, the primary reflectors are roughly spherical thus not breaking the azimuthal symmetry required by the meshes. Making wavefield adapted meshes ideal for large scale inversions
- Exploration scale surveys at the later stages are often reflection based and thus the aAMR meshes are not applicable for such studies.

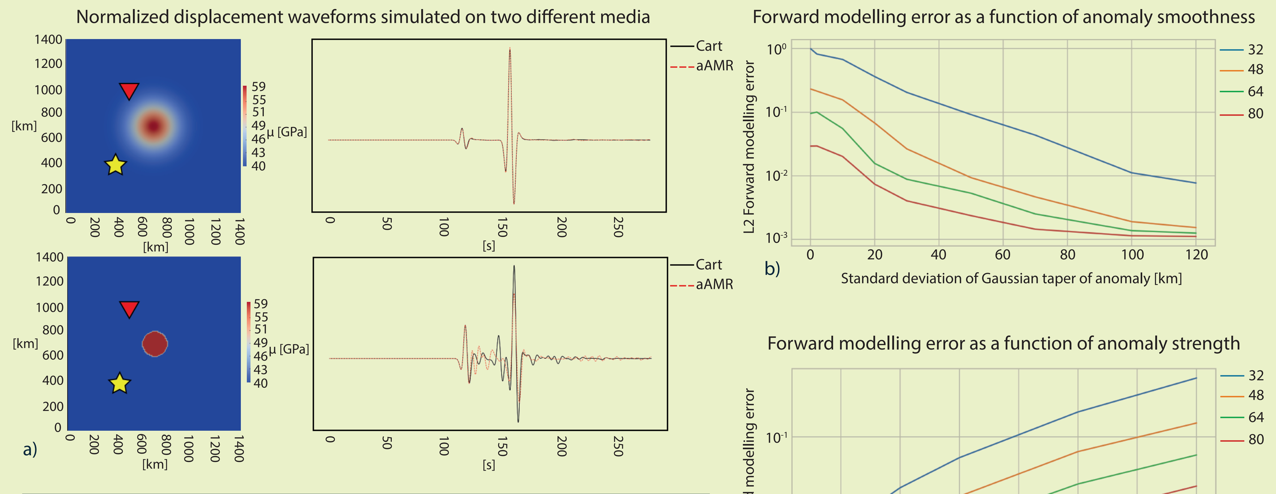

Figure 2. a) Normalized displacement waveforms recorded at the red triangle from a source at the yellow star. b) Forward modelling errors of varying aAMR meshes as a function of the standard deviation of the Gaussian taper of the 70 % anomaly. c) Same errors as in b) as a function of anomaly strength with a fixed smoothness of 10 km standard deviation of the Gaussian taper.

4. Frequency Scaling

- Given a homogeneous medium, the number of elements required by a standard meshing algorithm scales with frequency to the power of D, where D is the number of dimensions in the mesh.
- The wavefield adapted meshes have one dimension which is quasi independent of frequency which reduces the frequency scaling to a power of D-1.
- Results in a positive correlation between frequency and computational benefits.

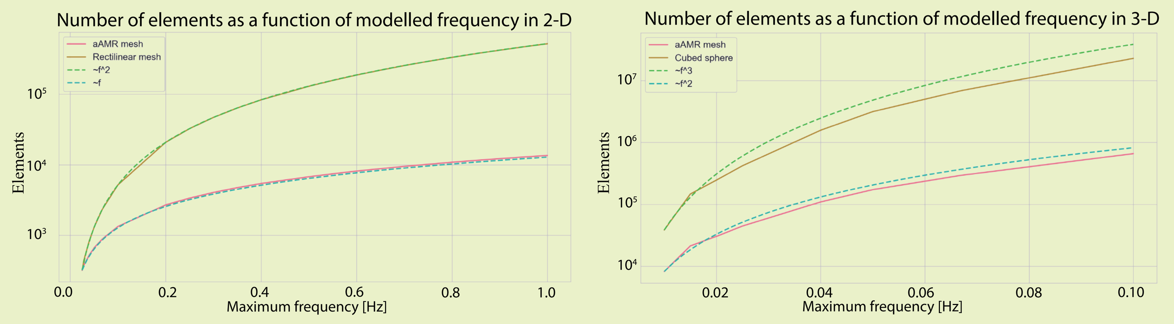

Figure 3. Number of elements needed to mesh a homogeneous medium with respect to frequency. Only strictly applies to homogeneous media.

5. Numerical Examples

- A comparison between a standard FWI and the proposed method in a 2D and 3D synthetic examples.
- A random medium with up to 8 % perturbations is recovered starting from a homogeneous model using 9 moment tensor sources with a minimum period of 10 s. Wavefield was recorded by 80 receivers.

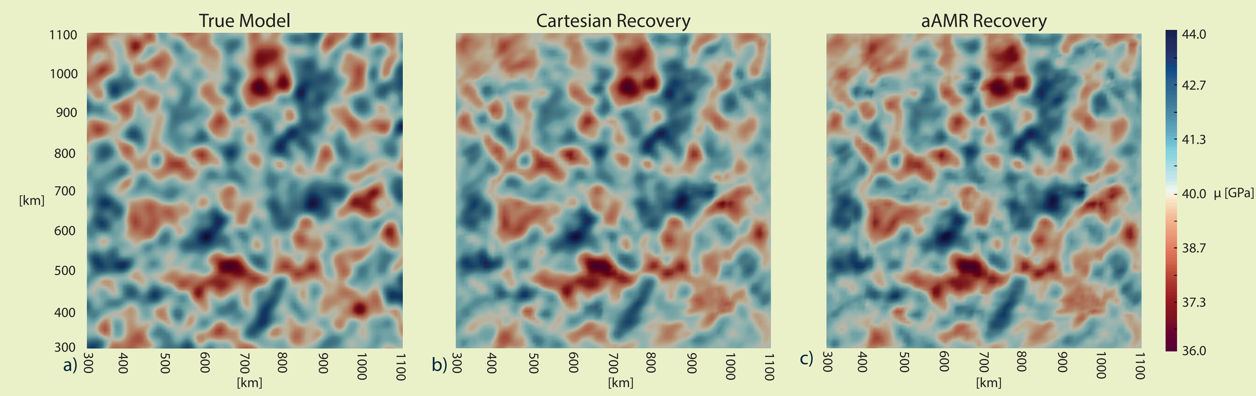

Figure 4. a) Shows the true medium. b) shows the medium recovered after 30 iterations using the regular Cartesian grid mesh and c) Shows the medium recovered after 30 iterations using aAMR meshes with 48 elements in the azimuthal direction.

- The same recovery was attempted for various number of azimuthal elements (Figure 5) and the performance is analysed in Figure 6.

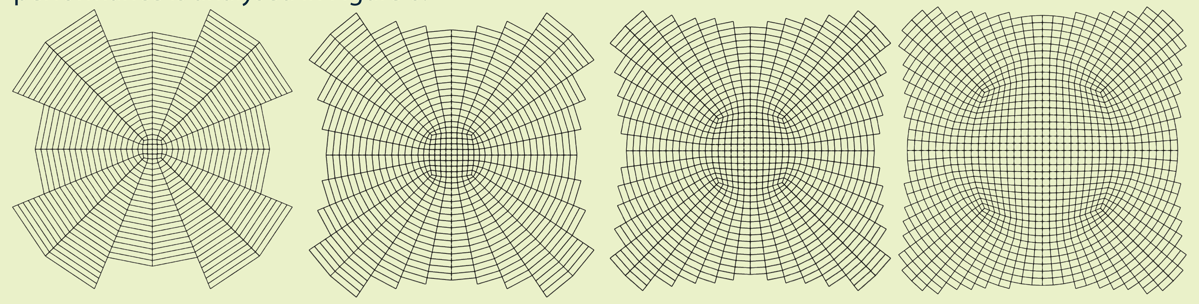

Figure 5. aAMR meshes with a varying number of elements in the azimuthal direction ranging from 16 - 80. The regular grid circles in the middle are bigger in these meshes than the ones used in the simulations.

- The number of azimuthal elements influences the quality of the recovery.
- As soon as the mesh is good enough, it can reconstruct a model of a similar quality and much lower computational cost.

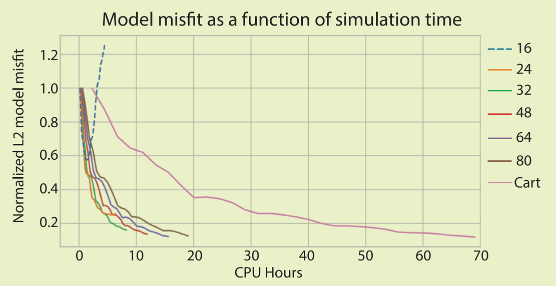

Figure 6. L2 model misfit between inverted model and true model normalized by the misfit between the homogeneous starting model and the true model.

- The method was tested in 3-D by reconstructing a smooth global chequerboard model with 10 % deviations from 1-D model.

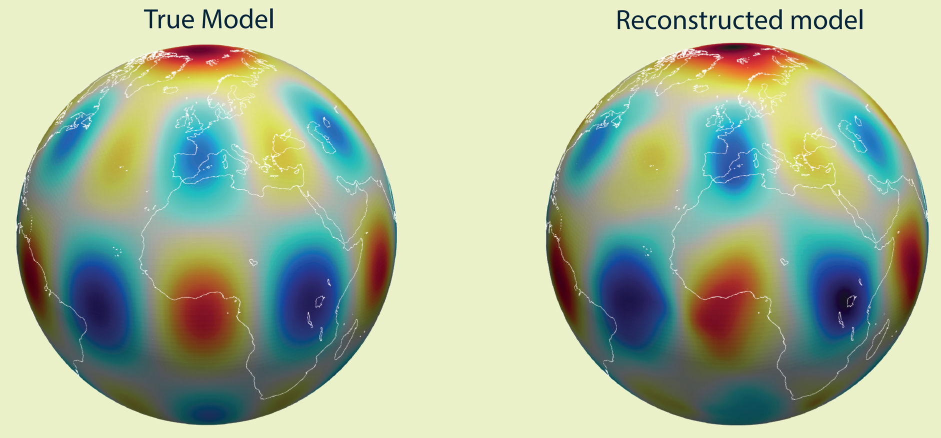

Figure 7. VS model snapshot comparison at 300 km depth.

- The model was reconstructed using a combination of the method presented by van Herwaarden et al. 2020 and Thrastarson et al. 2020. Starting model was 1-D and the cost of the reconstruction is equivalent to performing 1.6 standard FWI iterations.

6. Real Data

- An ongoing project is to apply this methodology to a real dataset. The project is still at its early stages
- We use an ever expanding dataset (currently at 500 earthquakes) and are in the process of creating a global FWI model.
- As the project is at its early stages, we can only show the results of a prototype inversion where we ran 8 mini-batch iterations starting from a modified version of PREM.
- The model was created with a total of 102 waveform simulations with a minimum period of 100 s.
- In spite of only being a prototype we can already detect some known features in the snapshot:
  - Afar region
  - West-African craton
  - Iceland hotspot
  - Azores hotspot

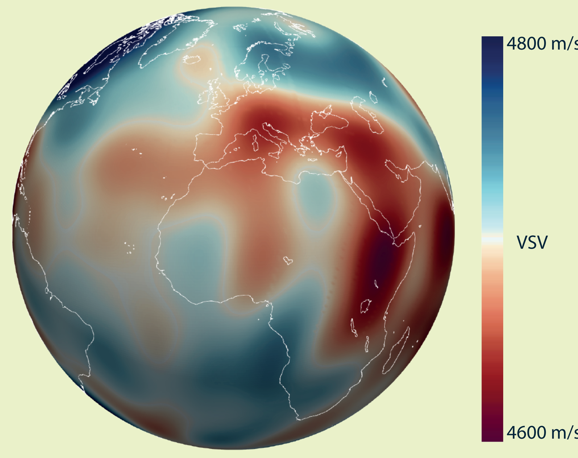

Figure 8. VSV model snapshot at 300 km depth.

- The prototype inversion gives a good indication that the methodology translates well from synthetics to real data and we will continue working in that direction.

7. Conclusion & Outlook

- The proposed method can deliver an order of magnitude reduction in FWI cost with minimal sacrifice in accuracy.
- Despite the adjoint wavefield being non-physical, the meshes still work to compute gradients accurately and efficiently.
- We are currently working towards applying this method on a real global scale inversion.

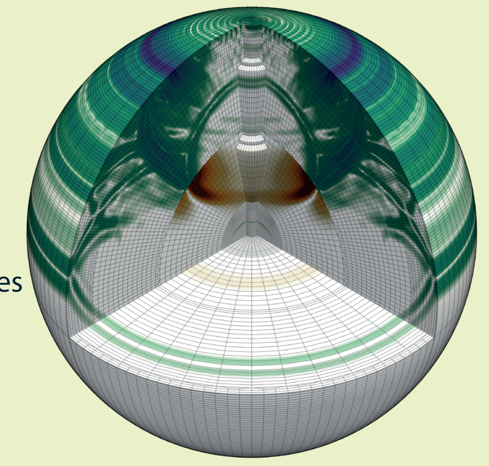

- For more information regarding wavefield adapted meshes in FWI: Thrastarson et al. GJI 2020 https://doi.org/10.1093/gji/ggaa065
- For more information regarding dynamic mini-batches: van Herwaarden et al. GJI 2020 https://doi.org/10.1093/gji/ggaa079

This work was supported by ERC grant #714069